Available online at www.sciencedirect.com

ScienceDirect

Procedia Structural Integrity 13 (2018) 1768–1773

Structural Integrity Procedia

www.elsevier.com/locate/procedia

ECF22 - Loading and Environmental effects on Structural Integrity

Implications of Substrate Geometry and Coating Thickness on the Cracking Resistance of Polymer-Based Protective Coatings

L A Wray[a], D Ayre[a], P E Irving[a], P A Jackson[b], P R Jones[c], F Zhao[c]

[a]*School of Aerospace, Transport and Manufacturing, Cranfield University, UK*
[b]*AkzoNobel Paints and Coatings, Felling, UK;* [c] *AkzoNobel Marine, Protective and Yacht Coatings, Felling, UK*

Abstract

Welded steel T-sections of different weld fillet geometries coated with water ballast tank protective coatings were subjected to thermal cycling with a temperature range from 60°C to -10°C. Cracks developed in the coatings at the weld line, propagating longitudinally along it. The number of cycles required to create 1 mm cracks was strongly dependent on the weld geometry and the coating Dry Film Thickness (DFT). Finite Element Modelling (FEM) was employed to calculate thermally induced strain fields in the coatings subjected to the same temperature range. FEM predicted that the greatest strain concentrations are present at the coating surface within the weld fillet region. Increased DFT and decreased fillet radius leads to increased maximum principal strains. Numerical analysis predicts that greatest strain ranges promoting the earliest cracking/failure are found in thicker coatings applied to smaller weld radii. Experimental observations confirm this.

Peer-review under responsibility of the ECF22 organizers.

Keywords: Coatings; Thermal Strains; Fatigue; FEM Analysis; Cracking Failure; Coating Life

1. Introduction

Corrosion is a common problem within the Marine industry. The deterioration of metal can affect the service life of structures and lead to premature failure. The increased maintenance costs and potential safety hazards that arise from Marine corrosion have resulted in a demand for high performance anti-corrosion coatings. An array of organic coatings have been developed to attempt to counter the effects of the corrosive Marine environment with mainly epoxy coating systems being developed for the protection of water ballast tanks (WBTs) on ships (Lee et al. 2013). In crude oil carriers these WBTs experience extreme environmental conditions caused by the variations in temperature between the crude oil being transported at approximately 60°C and the seawater pumped into the tank for ballast. This makes them particularly susceptible to coating failure (Park et al. 2007). Many studies into failure of WBT coatings have concluded that the most significant cracking is present in the weld fillet region of the stiffeners or where two planes

2452-3216
Peer-review under responsibility of the ECF22 organizers.
10.1016/j.prostr.2018.12.370

intersect at an angle (Mills & Eliasson 2006), (Zhou et al. 2012). Coating mechanical properties (Song et al. 2011), (Lee & Kim 2005) and thermo-mechanical properties (Zhang et al. 2005) have been measured and associated with cracking performance. Other investigations have considered strains caused by coating cure (Knudsen et al. 2006) and moisture absorption (Negele & Funke 1996) as possible driving factors for crack initiation.

The coating application conditions for WBT coatings are not ideal and it is known that the coating dry film thickness (DFT) is difficult to control. This results in a final thickness that can vary significantly from the manufacturer's specification. In their report Knudsen et al (2006) presented the intended and actual DFT of their test specimens and acknowledged that even under laboratory conditions there was a difference of up to 20% in measured DFT. The work of Zhang et al (2005) recognised that cracking resistance of epoxy coatings is dependent on DFT.

In this study the effect of weld geometry and DFT on the thermal fatigue lives of coatings on welded steel was investigated. This was achieved firstly by measuring the mechanical and thermal properties of the coating including strength, toughness and thermal expansion. Coating durability was assessed by thermally cycling welded steel T-sections with different weld geometries and different coating thickness. Crack development was monitored throughout the tests. Finite Element Modelling was employed to calculate thermally induced strain fields in coatings the weld.

2. Experimental Methods

2.1. Material Mechanical and Thermal Properties

The WBT coating selected for study was a highly filled epoxy. Young's modulus, strain to failure and fracture stress were measured on free film samples. These were produced by spraying the coating on to PTFE coated glass to produce a film of nominal DFT 300µm. This was cured at ambient for 7 days and post-cured at 100°C for 2 days to ensure the properties of the coating matched those achieved in service. Dogbone samples, Figure 1, were cut from the sheets after 2 days of ambient curing. Tensile testing was carried out at temperatures between -10°C and 60°C and stress-strain data extracted as described in an earlier paper (Wu et al. 2016). Young's modulus was determined from each stress-strain curve using a method based on ISO 527-1.

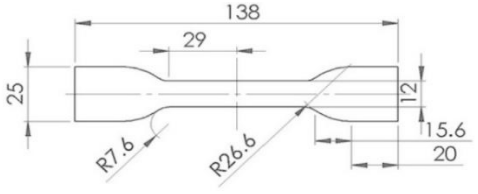

Figure 1: Dimensions (mm) of free film samples

Thermal properties were measured also using free film samples. The glass transition temperature (Tg) was determined using Differential Scanning Calorimetry on a section of thin film. Coefficient of Thermal Expansion (CTE) was measured on free film cylindrical samples approximately 5mm in diameter and height. These samples were tested using a Thermo-Mechanical Analyser under the process outlined by Wu (2015). The Tg of the coating was found to be 69±2°C. The results in Table 1 show that coating modulus decreases with increasing temperature while the strain to fracture increases. The CTE of the coating is 5 times larger than that of the steel substrate.

Table 1: Mechanical and thermal properties of coating (measured) and steel substrate (Wu 2015), (Cverna F. 2002).

Material	Temperature (°C)	Modulus (GPa)	Strain to Fracture (%)	Poisson's Ratio	CTE ($x10^{-5}$)
Steel Substrate	All	207	45	0.30	1.2
Coating	-10	6.3	0.27	0.31	6.0
	23	5.2	0.34		
	60	2.5	0.95		

2.2. Thermal cycling Sample Preparation

Welded T-sections were produced to represent the geometry of stiffeners found within WBTs. The sections were manufactured by MIG welding 6mm thick steel plates to give the sample geometry in Figure 2A. To investigate the effect of weld fillet geometry on coating life one of the welds on each T-section was milled to a constant 2mm radius.

The other side was kept as welded. Samples were then shot blasted to Sa2.5 standard. 5 samples were coated with a nominal DFT of 600µm and 2 were coated to a nominal DFT of 300µm. Once coated, samples were cured at room temperature for 7 days and post cured at 100°C for 2 days. DFT measurements on the flat surfaces of the samples were taken using an Elcometer 456 coating thickness gauge. The average DFT across all samples for the 600µm and 300µm variants was 578±68µm and 324±33µm respectively. The shape of the weld prevented measurements from being taken directly along the weld fillets. Sectioning of samples post testing revealed coating DFT on the milled weld fillets of the 300µm samples could be 6% greater than DFT on the flat and 36% greater on the non-milled welds. Sectioning of the 600µm samples showed DFT increases of 26% and 57% on the milled and non-milled welds respectively. The deflection of coated shims was used to measure thermal strains experienced by the coating on the flat areas of the T sections during thermal cycling. The measurement protocol was based on ASTM D6991-05 (2010). Thermal strains were measured throughout cycling and the results used in conjunction with the FEM analysis to estimate the maximum strains within the coated T-sections.

2.3. Thermal cycling

T-sections and coated shims were placed within an environmental chamber and subjected to thermal cycling. The thermal profile introduces 5-hour cycles from 60°C to -10°C and back to 60°C with ramp rates of 1°C/minute and 40minute temperature dwells at 60, 23 and -10°C. Thermocouples were used to verify that the chosen ramp rate would not result in any significant temperature lag between coating and substrate.

The T-sections were removed at intervals of approximately 30 cycles and inspected using a USB microscope. When cracks were identified an image was taken with scale present as shown in Figure 2B, the length of the crack was measured. The number of thermal cycles completed when the first 1 mm crack was observed was recorded for each sample.

2.4. Thermal cycling observations

Inspection of T-sections, removed at regular intervals, revealed cracks developing first in 600µm nominal DFT samples after 38 cycles. Cracks extended parallel to the weld length near the centre of the weld radii as illustrated in Figure 2A. At this stage cracking was identified only along non-milled welds. As thermal cycling progressed cracks developed on the milled welds of the same samples after 50 cycles. Further thermal cycling resulted in cracking in 300µm nominal DFT samples after 106 and 275 cycles for the non-milled and milled welds respectively. Inspection of cracks at increasing thermal cycles showed that cracks continued to grow as cycling progressed. Figure 2B illustrates the length of a single crack after 38, 64 and 171 thermal cycles. The cycles to achieve a 1 mm crack for each DFT variant and weld radius condition are presented in Figure 3.

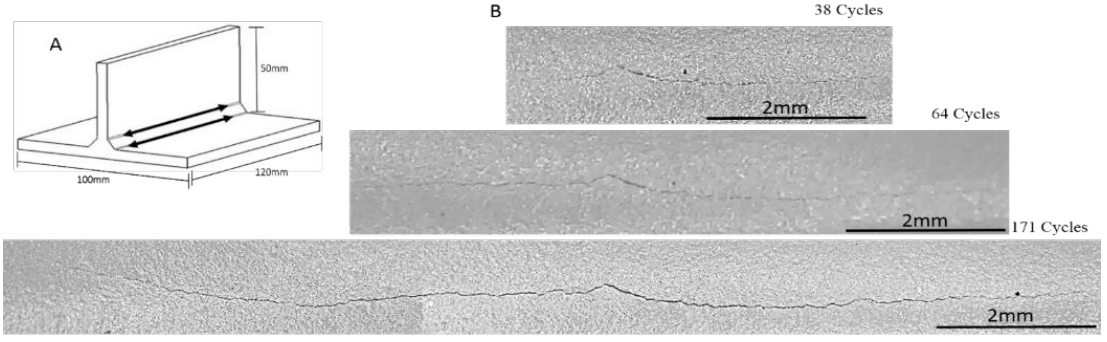

Figure 2: A - Illustration outlining the location and direction of channelling cracks observed;
B – Images of a single crack taken after 38, 64 and 171 thermal cycles taken from a 600µm nominal DFT variant non-milled weld.

Shim deflections to calculate thermal strain were measured at regular intervals during individual cycles at 60°C, 23°C and -10°C. During thermal cycling, as the samples are cooled from 60°C to -10°C the coating contracts and shim deflection is observed. As temperature increases the shim straightens with thermal strains tending towards zero. Figure 4 shows the average calculated thermal strains of 3 coated shims during cycles 10, 140 and 317. Strains of approximately 0.30±0.01% were observed at -10°C, with strains of 0.04±0.01% present at 60°C. Strain levels remained constant as thermal cycling progressed. This indicates that the coating applied to the flat surfaces of the steel

T-sections will experience a strain range of approximately 0.26% as the temperature is reduced from 60°C to -10°C.

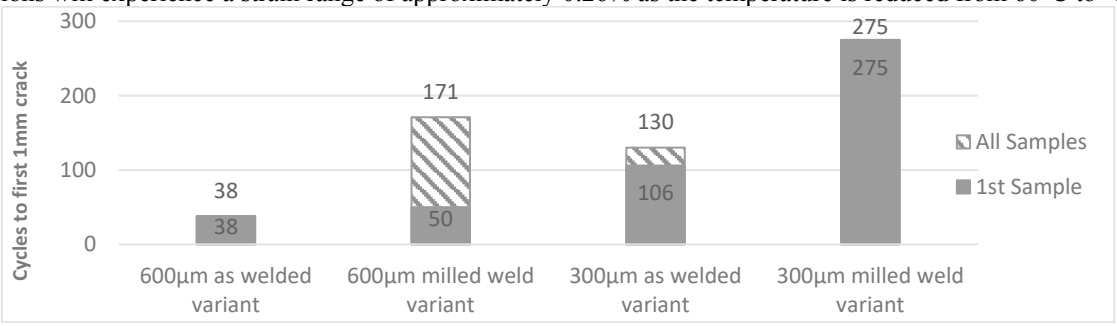

Figure 3: Cycles to first 1mm crack on thermal fatigue samples of varying DFT and weld condition

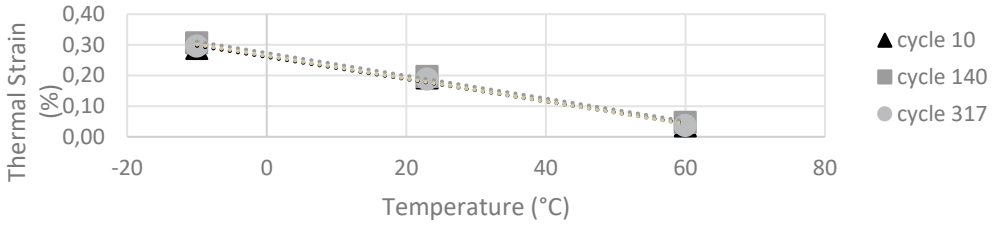

Figure 4: Average thermal strain measurements of 3 shims at thermal cycling intervals during 3 individual cycles

3. Finite Element Calculation of Thermal Strain

3.1. Model development

A 2D model was produced in Abaqus using deformable, planar shell elements. The part represented half a welded T-section partitioned to simulate coating/substrate sections. Substrate and coating sections were assigned the material properties shown in Table 1. As the maximum test temperature is below the Tg of the material only the CTE below Tg was input into the model. Principal stress directions were tangential and radial to the coating surface. Load steps were created with an initial temperature of 60°C followed by a ramp to -10°C that was consistent throughout the entire part. Standard, quadratic plane strain elements (CPE8R) were applied and a seed sensitivity study was carried out to identify ideal mesh conditions. A model simulating a 300µm DFT and 2mm weld fillet radius was analysed to understand the maximum principal stresses present in the coating at -10°C after the temperature had been reduced from 60°C. The results in Figure 5(Left) indicate that the largest stresses of 36MPa are in the centre of the radius along the tangential axis. This translates into a maximum strain of 0.39%. Strains present on the flat surfaces in the tangential direction equated to approximately 0.33%. However, this is significantly larger than the measured strain range presented in Figure 4, this discrepancy is currently under investigation. In the radial direction maximum strains were considerably lower, 0.08%. Therefore, in this situation the likely cause of coating failure is due to strains tangential to coating surface.

3.2. DFT and Weld Fillet Radius Analysis

The FE model was used to explore the effects of a wide range of coating DFT and weld fillet radii on the local strain concentrations in the coating. The data presented earlier in section 2.2 showed the measured DFT values to be between 300µm and 1000µm and radii to be from 0.5mm to 3mm. It can be concluded from the results that increasing DFT and decreasing radii will result in increased maximum strains in the weld region while strains on flat surface remained constant, independent of DFT. Comparing the strain in the weld fillet to the strain on the flat allowed a strain concentration factor to be determined for each condition. The results presented in Figure 5(Right) show that the strain concentration factor increases with increasing DFT and decreasing weld radius. These values may be applied to the measured experimental values of strain on a flat plate to estimate the maximum principal strains in coated T-sections.

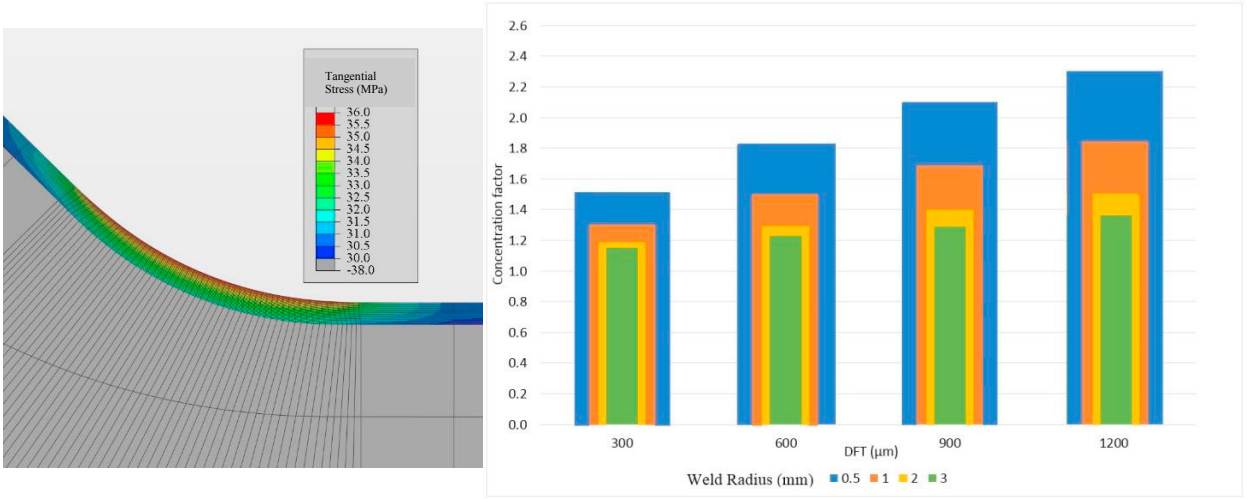

Figure 5: Left - Tangential stress in weld fillet radius at -10°C after a temperature reduction from 60°C; Right - Strain concentration factor in weld for varying DFT and weld fillet radius

4. Discussion

Thermal cycling of samples with varying weld fillet radii and coating DFT values demonstrate a relationship between coating geometry and thermal fatigue life. The first cracks were observed after 38 thermal cycles in the 600µm nominal DFT coatings along the non-milled welds, followed by cracks on the milled welds of these samples after 50 cycles. Measurements of local DFT presented in section 2.2 suggest values in the region of 1000µm. Applying the strain concentration factor (Figure 5(Right)) to the measured strain values (Figure 4) suggest that the local strains in the weld fillet for these samples at -10°C could be up to 0.6%. In the non-milled condition there could be greater variation in strain with the largest values being present in regions with a small radius. In contrast, samples with milled welds will have consistently lower DFT values and increased weld radii resulting in smaller local strains in the weld, and increased life. 300µm variants will have reduced local DFT values, in the region of 400µm, and therefore decreased maximum strains of up to 0.4%. This is consistent with the increased number of cycles to observed coating cracking, at 106 and 275 cycles for the non-milled and milled welds respectively.

A study by Wu (2017) on the same coating material applied to a steel substrate indicated a static strain to onset of first crack in the coating of 0.64±0.10%. Mechanical fatigue data showed that repeated application of 0.6% strain gave cycles to 2mm crack of less than 10. However, these samples were tested at ambient temperature and cannot be compared directly with the current thermal cycling results.Current studies are continuing the investigation to explore the failure mechanisms in similar materials under thermal cycling conditions.

5. Conclusions

1. Local strain levels in coatings on weld fillets under thermal cycling conditions are strongly dependent on local coating thickness and substrate weld fillet radius.
2. FE Modelling identified that strain concentrations will develop in the weld fillet region of a coated T-section. FEM predicts that coatings applied to smaller weld radii at an increased level of DFT will experience greater maximum principal strains within this weld region.
3. Thermal fatigue lives of welded T-sections are strongly dependent on local strain values at -10°C; greater DFT and reduced radius size will result in cracking after fewer thermal cycles.

Acknowledgements

The authors would like to thank AkzoNobel for support and supply of sample material, Cranfield University for

support to the project, and the Institute of Mechanical Engineers for financial support to attend ECF22.

References

ASTM D6991-05, 2010. Standard Test Method for Measurements of Internal Stresses in Organic Coatings by Cantilever (Beam). *Annual Book of ASTM Standards*, 05.

Cverna F., 2002. *Thermal Properties of Metals*, ASM International.

Knudsen, O. et al., 2006. Development of internal stress in organic coatings during cure and exposure. In *NACE International Corrosion Conference and Expo*.

Lee, C.-H., Han, K.-H. & Lee, S.-G., 2013. The effect of chlorinated seawater on coating performance of epoxy for a ship"s water ballast tank. In *NACE International Corrosion coference and expo*.

Lee, D.G. & Kim, B.C., 2005. Investigation of coating failure on the surface of a water ballast tank of an oil tanker. *Journal of Adhesion Science and Technology*, 19(10), pp.879–908.

Mills, G. & Eliasson, J., 2006. Factors influencing early crack development in marine cargo and ballast tanks. *JPCL*.

Negele, O. & Funke, W., 1996. Internal stress and wet adhesion or organic coatings. *Progress in Organic Coatings*, 28, pp.285–289.

Park, C.S. et al., 2007. Effects of surface preparation methods and protective coating types on the performance of erection joint weld seams in water ballast tanks. In *NACE International Corrosion Conference and Expo*.

Song, E. et al., 2011. Effect of coating formulation on crack resistance of epoxy coatings. In *NACE International Corrosion Conference and Expo*.

Wu, T. et al., 2017. Fatigue cracking behaviour of epoxy-based marine coatings on steel substrate under cyclic tension. *International Journal of Fatigue*, 99.

Wu, T. et al., 2016. Fracture of epoxy-based marine coatings as free films and substrated coatings under static tension. *Engineering Fracture Mechanics*.

Wu, T., 2015. *Investigation of the fracture behaviour of epoxy-based water ballast tank coatings under static and fatigue loadings*. PhD Thesis, Cranfield University.

Zhang, B.J. et al., 2005. Stress analysis and evaluation of cracks developed on the coatings for welded joints of water ballast tanks. In *NACE International Corrosion Conference and Expo*.

Zhou, G. et al., 2012. Experimental study of shrinkage of epoxy coating. In *15th International Conference on Experimental Mechanics*.

2018-12-31

Implications of substrate geometry and coating thickness on the cracking resistance of polymer-based protective coatings

Wray, Lesley-Anne

Elsevier

Wray LA, Ayre D, Irving PE, et al., Implications of substrate geometry and coating thickness on the cracking resistance of polymer-based protective coatings. Procedia Structural Integrity, Volume 13, 2018, pp. 1768-1773

https://doi.org/10.1016/j.prostr.2018.12.370